HHS Public Access

Author manuscript

Life Sci Space Res (Amst). Author manuscript; available in PMC 2020 March 10.

Published in final edited form as:

Life Sci Space Res (Amst). 2018 May ; 17: 51–62. doi:10.1016/j.lssr.2018.03.004.

Late Effects of ^{1}H Irradiation on Hippocampal Physiology

Frederico Kiffer[a,b], **Alexis K. Howe**[a,b], **Hannah Carr**[a,b], **Jing Wang**[a,b], **Tyler Alexander**[a,b], **Julie E. Anderson**[a,b], **Thomas Groves**[a,b,c], **John W. Seawright**[a,b], **Vijayalakshmi Sridharan**[a,b], **Gwendolyn Carter**[a,b], **Marjan Boerma**[a,b], **Antiño R. Allen**[a,b,c]

[a]Division of Radiation Health, University of Arkansas for Medical Sciences, Little Rock, AR 72205

[b]Department of Pharmaceutical Sciences, University of Arkansas for Medical Sciences, Little Rock, AR 72205

[c]Neurobiology & Developmental Sciences, University of Arkansas for Medical Sciences, Little Rock, AR 72205

Abstract

NASA's Missions to Mars and beyond will expose flight crews to potentially dangerous levels of charged-particle radiation. Of all charged nuclei, ^{1}H is the most abundant charged particle in both the galactic cosmic ray (GCR) and solar particle event (SPE) spectra. There are currently no functional spacecraft shielding materials that are able to mitigate the charged-particle radiation encountered in space. Recent studies have demonstrated cognitive injuries due to high-dose ^{1}H exposures in rodents. Our study investigated the effects of ^{1}H irradiation on neuronal morphology in the hippocampus of adult male mice. 6-month-old mice received whole-body exposure to ^{1}H at 0.5 and 1Gy (150 MeV/n; 0.35-0.55Gy/min) at NASA's Space Radiation Laboratory in Upton, NY. At 9-months post-irradiation, we tested each animal's open-field exploratory performance. After sacrifice, we dissected the brains along the midsagittal plane, and then either fixed or dissected further and snap-froze them. Our data showed that exposure to 0.5 Gy or 1 Gy ^{1}H significantly increased animals' anxiety behavior in open-field testing. Our micromorphometric analyses revealed significant decreases in mushroom spine density and dendrite morphology in the Dentate Gyrus, Cornu Ammonis 3 and 1 of the hippocampus, and lowered expression of synaptic markers. Our data suggest ^{1}H radiation significantly increased exploration anxiety and modulated the dendritic spine and dendrite morphology of hippocampal neurons at a dose of 0.5 or 1 Gy.

Keywords

behavior; hippocampus; neuron; morphology; radiation; space

1. INTRODUCTION

NASA's efforts to continue manned space exploration over the next two decades includes a mission to Mars in the late 2030s, preceded by several Deep Space Gateway missions where

*Address for corresponding author: Dr. Antiño R. Allen, University of Arkansas for Medical Sciences, 4301 West Markham, Suite 441B-2, Little Rock, AR 72205, Phone: 501-686-7553; Fax: 501-526-6599; Aallen@uams.edu.

Competing Interest: None of the authors has competing financial interests or other conflicts of interest.

humans will be subjected to the deep-space radiation environment without protection from Earth's magnetosphere for extended periods of time. Projected round-trip missions to Mars will range from 560 to 1,100 days depending on launch windows and final mission design.[1] Data from *Curiosity* on Mars and aboard its transit vehicle, the *Mars Science Laboratory* have provided an approximate total dose equivalent for an 850 day mission near solar maximum of approximately 1.01Sv.[2,3]

The biological challenges presented by a manned mission to Mars are unique as humans have never been exposed to microgravity or the complex field of the high-energy charged particles comprising the deep-space radiation environment for the duration of multiple years before. Charged particle radiation in deep space originates either from galactic cosmic rays (GCR), which provide a constant exposure, or solar particle events (SPE), which modulate according to the 12-year solar cycle.[4] High-energy protons (^{1}H) are the most abundant charged particle in the deep-space environment, constituting approximately 85% of GCR, and the majority of ejected coronal plasma during SPE.[4,5] In addition, SPE are extraordinarily dangerous in that discriminate events are currently unpredictable, and are capable of delivering a high dosage in a short period of time. ^{1}H alone deliver approximately 50-60% of the constant total organ dose due to GCR exposure in deep space.[6]

NASA has adopted a permissible exposure limit for its personnel such that a lifetime risk of death due to work exposure cannot exceed 3% on a 95% confidence interval. This limitation places the lifetime risk of death of astronauts due to radiation on one mission to Mars at approximately three times the current limit. However, risk estimates due to deep-space radiation are currently based on radiation-induced carcinogenesis, damage to blood forming organs, skin and lens, most of which would likely manifest several years after return.[6] Recent evidence shows that charged particle radiation induces deficits on organ systems such as the circulatory, immune and central nervous systems (CNS). The possible acute CNS risks to in-flight radiation exposure include motor, cognitive and social deficits, which provide serious concerns for in-flight complications, potentially compromising a mission. In addition, there is also concern for the long-term welfare of astronauts, whose CNS may undergo premature aging, and amyloid-β buildup upon return.[4,6-8]

NASA's risk-factor modeling for radiation-induced detriments to the CNS correspond to the hippocampus, which is vital to the processes of memory consolidation, retrieval, and executive function.[6,9] The stochastic nature of charged particle interactions with normal tissues presents a challenge in predicting biological outcomes due to irradiation. However, recent *in silico* work involving the interactions of cross-sections via Monte-Carlo simulations with neurons suggests dendritic spine and neurogenesis sensitivity to charged-particle radiation.[10-12] Indeed, various *in vivo* studies are beginning to categorize the resulting changes in micromorphologies of hippocampal neurons in response to charged particles of different dosages, energies and atomic number. Recent publications reveal changes in dendritic complexity, length, branching, volume, and spine subtypes.[13-15] In addition, there is evidence of radiation-induced insults to neurogenesis in the granule cell layer of the dentate gyrus (DG).[16-18] Furthermore, high-energy charged particles appear to alter the striatal dopaminergic system associated with some motor and learning processes.[19,20]

The processes of memory formation and retrieval are multi-faceted and complex. In this respect, no morphological or molecular experiment can yet single-handedly define cognitive deficits in irradiated animals despite similarities in neurological diseases and radiation treatment. Yet, some studies examining morphological and molecular changes to hippocampal and prefrontal cortex neurons as a result of high-energy ^{1}H irradiation ultimately show behavioral deficits in cognitive task paradigms. Rats exposed to 3 and 4 Gy (250 MeV/n) failed to recognize a novel object in the novel object recognition (NOR) paradigm as well as reduced habituation to acoustic startle and acute learning up to 12 weeks.[21] Mice exposed to doses of 0.5 or 2 Gy (150 MeV/n) showed deficits in the NOR and Object-in-Place tests at 1-month after radiation and mice irradiated at 0.5 Gy (150 MeV/n) displayed reversal learning deficits in the Morris Water Maze (MWM) paradigm.[22,23] NOR deficits have been observed even at the low dose of 0.1 Gy (150 MeV/n) three months postexposure in mice.[24] However, not all studies examining behavioral changes due to ^{1}H show deficits in cognitive behavior. Rats exposed to 1.5, 3 and 4 Gy (250 MeV/n) showed no changes in conditioned taste aversion, or spatial learning via the MWM.[25] Mice treated with 2 Gy (150MeV/n) showed no signs of impaired spatial learning or memory in the MWM task, and a study examining changes in a bar press task in rats irradiated at 4 Gy (250 MeV/n) reports no changes due to treatment.[26,27] This study reports behavioral, morphological and molecular changes to granular and pyramidal neurons of the hippocampus as a result of exposure to ^{1}H at 0.5 or 1 Gy (150MeV/n) at the novel time point of 9 months post exposure.

2. MATERIALS AND METHODS

2.1 Animals and Irradiation

The Institutional Animal Care and Use Committees of the University of Arkansas for Medical Sciences (UAMS) and Brookhaven National Laboratory (BNL) have approved all procedures outlined in this publication. Male C57BL/6 mice were obtained from Jackson Laboratory (Bar Harbor, ME) and were housed 5 per cage. Throughout the duration of the study, mice received standard rodent chow that was low in soy (2020X, Harlan Laboratories), water ad libitum, and were housed on a 12:12 hour light:dark cycle. At 6 months of age, mice were transported to BNL by overnight airlift. At BNL, mice were again administered the 2020X diet, water *ad libitum*, and were housed on a 12:12 hour light:dark cycle. After a one week acclimation, mice were exposed to whole-body irradiation at the NASA Space Radiation Laboratory (NSRL) at BNL. For this purpose, mice were individually placed in well-ventilated clear Lucite cubes, and then placed within the NSRL beam line, 5 mice at the time. Mice received a single dose of ^{1}H (150 MeV, 0.5 Gy, 0.35-0.55 Gy/min), and immediately after exposure, mice were placed back in their cage. Radiation dosimetry was performed by the NSRL physics team. Sham-irradiated mice were also transported to NSRL and placed in clear Lucite cubes, but were not exposed to ^{1}H. Two days after irradiation or sham treatment, mice were returned to UAMS by overnight airlift. Upon return, mice were administered 2020X chow, containing 150 ppm fenbendazole, for 8 weeks, as a routine UAMS quarantine procedure.

2.2 Behavioral Testing

Behavioral testing was performed 9 months after irradiation. Animals underwent behavioral testing for the open field paradigm, a two day procedure in which animals freely explore an empty arena for ten minutes each day. Animals are placed in the center of the arena and measures of locomotor activity and animal location are taken for the duration of the session. The arena is a cube consisting of an aluminum floor, opaque leucite walls and an open ceiling. The arena was wiped clean with 20% EtOH solution after each trial. Each session was recorded on a charge-coupled device video camera, located above the maze for automatic behavioral analysis with EthoVision software version 11 (Noldus Information Technology).

2.3 RNA Extraction and Quantitative Reverse Transcription Polymerase Chain Reaction (qRT-PCR)

9 months after irradiation, mice were anesthetized by isoflurane inhalation, and hippocampi were dissected from each treatment group (n=10), immediately frozen in liquid nitrogen, and subsequently stored at −80°C. Total RNA was extracted from hippocampal tissue with the AllPrep DNA/RNA extraction kit (QIAGEN, Valencia, CA), according to the manufacturer's protocol. RNA quality and quantity was assessed on a Nanodrop 2000 instrument (Thermo Scientific, Waltham, MA). cDNA was synthesized with random primers and a high-capacity cDNA reverse transcription kit (Applied Biosystems, Foster City, CA), according to the manufacturer's protocol (Life Technologies, Grand Island, NY). The levels of gene transcripts were determined by qRT-PCR with TaqMan Gene Expression Assays (Life Technologies, and Integrated DNA Technologies, Coralville, IA), according to the manufacturer's protocol. In all cases, GAPDH was used as an internal reference gene, and fold changes were calculated with the 2-ddCt method. Measurements were taken in duplicates.

2.4 Golgi Staining

To establish the impact of ^{1}H on mature neuronal morphology, brains from mice exposed to ^{1}H were Golgi stained and analyzed for structural changes in hippocampal neurons. Advantages of the Golgi–Cox method for assessing dendritic spine dynamics are its resistance to fading or photobleaching over time. Often cited disadvantages of Golgi–Cox staining are the limited ability to determine the neurochemical phenotypes of impregnated neurons and inability to image smaller spine subtypes such as filopodia. However, the Golgi-Cox method has been described as a useful tool in a variety of human diseases and animal models, where data from gross inspection or histology was not consistent with the expected behavioral/neurologic alteration.[28,29]

Immediately after sacrifice, brains (n = 5-6) were extracted and bilaterally cut along the mid-sagittal plane, then brains were treated with the Golgi-Cox method of staining. Right hemispheres were immersed for 2 weeks in an impregnation solution containing potassium dichromate and mercuric chloride. Samples were then immersed for at least 48 hours in a post-impregnation buffer. Each sample was sectioned at 200 μm in 1X PBS with a microtome. Samples were then transferred into wells and washed with 0.01 M PBS buffer (pH 7.4) with Triton X-100 (0.3%) (PBS-T). Immediately after washing, samples were

stained with ammonium hydroxide and then immersed in a post-staining buffer (Bioenno Tech superGolgi kit). Sections were again washed in PBS-T, mounted on 1% gelatin-coated slides, and allowed to dry. Sections were finally dehydrated with ethanol solutions, followed by cleaning in xylene, and coverslipped with Permount™ (Fisher).

2.5 Dendritic Spine Density and Spine Morphology

Blinded to the experimental conditions, we analyzed dendritic spines that were conducted on coded Golgi impregnated brain sections which contained the dorsal hippocampus for the dentate gyrus (DG) and CA1. Spines were examined on dendrites of the DG granule neurons as well as apical (stratum radiatum) and basal (stratum oriens) dendrites of CA1 pyramidal neurons. The neurons that satisfied the following criteria were chosen for analysis in each of the experimental groups: presence of 1) non-truncated dendrites; 2) consistent and dark Golgi staining along the entire extent of the dendrites; and 3) relative isolation from neighboring neurons to avoid interference with analysis.[30] Five dendritic segments (each at least 20 nm in length[31]) per neuron were analyzed, and 6-7 neurons were analyzed per brain. Neurons that met staining criteria were traced using a 100 X oil objective, a computerized stage, and Neurolucida software (Ver. 11, Microbrightfield, Inc., Williston, VT).

2.6 Dendritic Morphology Quantification

We explored morphological characteristics using techniques that included Sholl analysis, total dendritic length, number of branch points, and dendritic complexity index (DCI); these were performed with the Neuroexplorer component of the Neurolucida program. First, we collected the Sholl analysis, which is used to assess the amount and distribution of the arbor at increasing radial distances from the cell body.[32] We set the distance between each radius to 10 μm for our experiments. The length of each dendritic branch, within each progressively larger circle, is counted from the soma. This provides information about the amount and distribution of dendritic material.

Next, we performed branch-point analyses. A branch point represents a bifurcation of the dendrite when a branch divides into two sub-branches. Branch-point analysis is based on the number of bifurcations and the order of the points.[33] Lower branch-point orders represent proximal regions of the tree, whereas larger branch-point orders characterize distal regions. We used the branch-point analysis to determine the complexity of the dendritic arborization because the complexity of the dendritic tree is an important phenotypic component of the branching analysis. DCI was determined by the following equation, DCI=∑branch tip orders + # branch tips) x (total dendritic length/total number of primary dendrites). In the CA1 areas, apical and basal dendrites were analyzed separately.

2.7 Statistical Analysis

We expressed data as a mean ± the standard error of the mean (SEM). A one-way ANOVA followed by a post-hoc Bonferroni correction for multiple comparisons was employed for total distance moved in open field testing. Behavioral heat maps corresponded to animals' center points and represent mean locations for all animals in each cohort. To evaluate statistical differences in NMDA/AMPA receptor, synaptic marker, and cytokine mRNA expression between sham and irradiated groups, we used a one-way ANOVA followed by

Newman-Keuls multiple corrections tests. All statistical analyses were conducted with GraphPad Prism 6.0 software (La Jolla, CA), and $p < 0.05$ was considered significant. For measures of dendritic intersections, we used a mixed-factors ANOVA to test for the effects of irradiation (between subjects variable) and distance from the cell body (Sholl radius, repeated measures variable), and then conducted Fisher least significant difference post-hoc tests, when appropriate.

3. RESULTS

3.1 Behavioral Testing

We used the open-field paradigm to assess anxiety in exploratory behavior.[34] First, we analyzed the activity of the mice in the novel enclosure on training days 1 and 2. Our results indicate an effect of treatment on day 2 locomotion ($F_{(2, 25)} = 24.36$; $p < 0.0001$). Post hoc analysis revealed that the average distance moved was significantly reduced in both treatment groups during testing (Sham vs 0.5 Gy $p < 0.0001$; Sham vs 1 Gy $p < 0.0001$; Fig. 1a).

When placed in an open arena, mice generally prefer remaining near the walls, a tendency dubbed thigmotaxis. Thigmotaxis gradually decreases in untreated mice as they familiarize with the arena, resulting in more exploration of the center of the arena. Anxiolytic drugs have demonstrated increased thigmotaxis relative to untreated mice.[35] We observed pronounced thigmotaxis in animals irradiated at 0.5 and 1 Gy on both open-field testing days (Fig. 1b).

3.2 Changes in Spine Density and Spine Morphology

The quantitative analysis showed that radiation increased the overall spine density in the DG ($F_{(2, 32)} = 5.18$, $p < 0.05$; Table 1). Analyses of the density of different spine types indicated that radiation had a significant effect of treatment ($F_{(2, 31)} = 3.22$, $p < 0.05$; Table 1). Post hoc analysis revealed that relative to the sham group, 0.5 Gy ^{1}H significantly increased density of stubby spines (Sham vs 0.5 Gy, $p < 0.05$). Irradiation also significantly modulated mushroom spine density ($F_{(2, 32)} = 8.34$, $p < 0.01$; Table 1). Holm-Sidak analysis revealed 1 Gy ^{1}H significantly decreased density of mushroom spines (Sham vs 1 Gy, $p < 0.001$; Table 1). There were no significant change in the overall density of thin spines ($F_{(2, 32)} = 2.30$, $p = 0.12$).

There were no significant changes in the overall density of spines in the CA1 apical pyramidal dendrites ($F_{(2, 15)} = 0.04$, $p = 0.96$). When we analyzed the density of different types of dendritic spines, we found that the density of mushroom spines decreased dramatically ($F_{(2, 15)} = 4.45$, $p < 0.05$;). Holms-Sidak analysis revealed 1 Gy ^{1}H significantly decreased density of mushroom spines (Sham vs 1 Gy, $p < 0.05$; Table 2). Surprisingly, there was significant increase in the proportion of thin spines ($F_{(2, 15)} = 7.62$, $p < 0.01$; Table 2) in mice exposed to 1 Gy. We found no significant difference in the density of stubby spines ($F_{(2, 15)} = 1.54$, $p = 0.25$; Table 2).

In the basal pyramidal dendrites of the CA1 region, overall spine density was also unchanged after irradiation ($F_{(2, 14)} = 2.80$, $p = 0.09$). When we analyzed spine morphology,

there were significant effect of ^{1}H radiation on mushroom ($F_{(2, 14)} = 6.18$, $p < 0.05$) spines. Holms-Sidak analysis revealed 1 Gy ^{1}H significantly decreased density of mushroom spines (Sham vs 1 Gy, $p < 0.01$; Table 2). We found no significant difference in the density of stubby spines ($F_{(2, 15)} = 1.54$, $p = 0.25$).

Similar to what was seen in the CA1 apical pyramidal dendrites, there were no significant changes in the overall density of spines ($F_{(2, 12)} = 0.33$, $p = 0.72$) in CA3. Next we analyzed spine morphology. There were significant effects of radiation on mushroom spines ($F_{(2, 13)} = 5.78$, $p < 0.05$). Post hoc analysis revealed 1 Gy ^{1}H significantly decreased density of mushroom spines (Sham vs 1 Gy, $p < 0.05$; **see** Table 3). In the CA3 basal pyramidal dendrites, there was no significant change in the overall density of spines ($F_{(2,13)} = 1.53$, $p = 0.25$). In addition, there was no significant changes in mushroom spines ($F_{(2,13)} = 1.91$, $p = 0.19$; **see** Table 3), stubby ($F_{(2,13)} = 2.18$, $p = 0.15$) or thin spines ($F_{(2,12)} = 1.91$, $p = 0.19$; **see** Table 3) compared to sham.

3.3 Dendritic morphology

3.3.1 Dentate gyrus granule neurons—To investigate the effects of ^{1}H irradiation on neuronal morphology, we performed a segmental Sholl analysis to examine the changes in dendritic length as a function of radial distanced from the cell soma. There was a significant interaction between treatment and Sholl dendritic intersections after 0.5 Gy ($F_{(26,208)} = 6.48$; $p<0.0001$) and 1 Gy ($F_{(26,208)} = 2.72$; $p < 0.0001$) in the DG, indicating that effect of radiation is associated with a different distribution of dendritic branches over the entire tree. The ANOVA also detected significant main effects of Sholl dendritic intersections after 0.5 Gy ($F_{(26,208)} = 152.5$; $p <0.0001$) and 1 Gy ($F_{(26,208)} = 137.0$; $p<0.0001$). Post hoc analysis revealed that radiation decreased dendritic arborization compared to the sham controls. This decrease in arborization was particularly evident after 0.5 Gy at 20 - 50 μm from the soma (Fisher's LSD, $p<0.01$), then 60 - 120 μm (Fisher's LSD, $p<0.0001$; Fig. 2a), and 130 μm (Fisher's LSD, $p<0.01$). However, there was an increase in arborization mice exposed to 1 Gy at the distance between 130 μm from the soma (Fisher's LSD, $p<0.05$), 140 μm (Fisher's LSD, $p<0.01$), 150 μm (Fisher's LSD, $p<0.05$), then 160 - 190 μm (Fisher's LSD, $p<0.05$; Fig. 2b) from the soma.

In addition, differences were found in total dendritic length after radiation ($F_{(2, 12)} = 14.48$, $p< 0.001$; Table 4). Multiple comparison test revealed this was driven by a significant decrease in mice exposed to .5 Gy ($p<0.05$) compared to sham and in the number of branch points ($F_{(2, 11)} = 33.28$, $p < 0.0001$; Table 4). The DCI of the DG, which is calculated from the parameters, was significantly different between the groups after radiation ($F_{(2, 12)} = 12.94$, $p < 0.001$; Table 4).

3.3.2 CA1 pyramidal neurons—A similar analysis was performed on the apical and basal region of the CA1 pyramidal neurons. There was a significant interaction between irradiation and segmental dendritic Sholl intersections in the CA1 apical area in the 1 Gy ($F_{(26,208)} = 1.55$: $p<0.05$), but not in the 0.5 Gy ($F_{(26,208)} = 1.28$; $p = 0.17$) treatment group. However, the ANOVA also detected a significant main effect of dendritic length after 0.05 Gy ($F_{(26,208)} = 79.39$; $p <0.0001$) and 1 Gy ($F_{(26,208)} = 104.0$; $p<0.0001$). Post hoc analysis

revealed that ^{1}H radiation reduced dendritic arborization compared to the sham controls. This decrease in arborization was particularly evident after 0.5 Gy at 80 - 110 μm from the soma (Fisher's LSD, $p<0.05$; Fig. 3a). There was also a decrease in arborization in mice exposed to 1 Gy at the distance between 120 - 130 μm from the soma (Fisher's LSD, $p<0.05$; Fig. 3c).

In contrast to what was seen in the CA 1 apical, there were no significant interactions in the basal CA1 between irradiation and segmental dendritic Sholl intersections for 0.5 Gy ($F_{(26,208)} = 1.07$; $p = 0.37$) or 1 Gy ($F_{(26,208)} = 1.17$; $p = 0.26$). However, the ANOVA also detected significant main effect of dendritic length after 0.5 Gy ($F_{(26,208)} = 198.8$; $p <0.0001$) and 1 Gy ($F_{(26,208)} = 117.0$; $p<0.0001$). Post hoc analysis revealed that radiation reduced dendritic arborization compared to the sham controls. This decrease in arborization was particularly evident after 0.5 Gy at 40 - 60 μm (Fisher's LSD, $p<0.05$; Fig. 3b). There was also a decrease in mice exposed to 1 Gy at the distance between 50 - 80 μm from the soma (Fisher's LSD, $p<0.05$; Fig. 3d).

Similar to the observation in the DG, we found differences in the CA1 apical areas for total dendritic length after radiation (Apical $F_{(2, 12)} = 4.65$, $p < 0.05$; Table 5), the number of branch points (Apical $F_{(2, 12)} = 8.18$, $p < 0.01$; Basal $F_{(2, 12)} = 4.54$, $p < 0.01$; Table 5), and the branch point complexity (Apical $F_{(2, 1)} = 4.28$, $p < 0.05$ Table 5).

3.3.3 CA 3 pyramidal neurons—There was no significant interaction between radiation and Sholl dendritic interactions in the CA3 Apical area for 0.5 Gy ($F_{(26,208)} = 0.50$; $p = 0.97$; Fig 4a) and for 1 Gy ($F_{(26,208)} = 1.23$; $p = 0.21$; Fig 4c). In the CA 3 basal, the ANOVA detected significant interaction between irradiation and sholl dendritic intersections in the 0.5 Gy treated ($F_{(26,208)} = 4.20$; $p < 0.0001$). Post hoc analysis revealed decreases in arborization was particularly evident after at 30 - 40 μm from the soma (Fisher's LSD, $p<0.05$) then 100 - 200 μm (Fisher's LSD, $p<0.01$; Fig 4b) and 210 μm (Fisher's LSD, $p<0.05$). In the 1 Gy exposed mice the ANOVA detected significant interaction between irradiation and sholl dendritic intersections ($F_{(26,208)} = 4.00$; $p < 0.0001$) and an effect of length ($F_{(26,208)} = 70.61$: $p<0.001$). Post Hoc analysis revealed that 1 Gy radiation reduced dendritic arborization at 30 - 40 μm from the soma (Fisher's LSD, $p<0.05$) then 100 - 180 μm (Fisher's LSD, $p<0.01$; Fig 4d)> and 190 μm (Fisher's LSD, $p<0.05$) compared to the sham controls.

No differences were found in the CA3 apical area for total dendritic length (Apical $F_{(2,10)} = 2.09$, $p < 0.12$), but there was a significant difference in basal ($F_{(2,12)} = 2.09$, $p < 0.05$). When sham were compared to 0.5 and 1Gy irradiated mice there were no significant difference number of branch points (Apical $F_{(2,11)} = 0.81$ $p = 0.46$; Basal $F_{(2,12)} = 3.43$ $p = 0.06$; Table 6), or in overall complexity (Apical $F(2,11) = 0.37$ $p = 0.37$; Basal $F(2,12) = 2.61$ $p = 0.11$; Table 6).

3.4 Changes in mRNA expression

3.4.1 NMDA/AMPA Subunits—We examined the mRNA expression of glutamate receptors in response to radiation. N-methyl-D-aspartate (NMDA) subunit Nr1 underwent a dose-dependent reduction in expression ($F_{(2,24)}=10.30$, $p<0.001$; Fig. 5a). Furthermore, the

multiple comparisons test reveals significant decreases from sham to 0.5 Gy ($p<0.05$; Fig. 5a), 0.5 Gy to 1 Gy ($p<0.05$; Fig. 5a) and from sham to 1 Gy ($p<0.001$; Fig. 5a). α-amino-3-hydroxy-5-methyl-4-isoxazole propionic acid (AMPA) subunit GluR1 also resulted in a dose-dependent decrease in mRNA expression ($F_{(2,24)}=6.17$, $p<0.01$; Fig 5b). Additionally, multiple comparisons show a significant decrease in expression from sham to 0.5 Gy ($p<0.05$: Fig 5b) and from Sham to 1 Gy ($p<0.01$; Fig 5b).

3.4.2 Synaptic Markers—We analyzed the mRNA expression of presynaptic marker synapsin-1 (Syn1) and postsynaptic marker Synapse-Associated Protein 97 (SAP-97). Animals irradiated with 1 Gy underwent down-regulation of Syn 1 ($F_{(2,32)}=12.92$, $p<0.0001$; Fig. 5c). Post-hoc multiple comparisons indicate a decrease from sham to 1 Gy ($p<0.001$) and from 0.5 Gy to 1 Gy ($p<0.001$; Fig. 5c). Inversely, the postsynaptic scaffolding protein SAP-97 appears to have been up-regulated in both cohorts of irradiated animals ($F_{(2,32)}=12.92$, $p<0.0001$; Fig. 5d). Significant increases from sham to both 0.5 Gy and 1 Gy were also revealed from multiple comparisons ($p<0.05$; Fig. 5d).

3.4.3 Microglia—In order to determine the immune response to ^{1}H irradiation in the brain, we quantified the mRNA content of microglial phenotypic markers. CD68 mRNA, a marker for activated microglia, resulted in a dose-dependent increase ($F_{(2,23)}=20.19$, $p<0.0001$; Fig. 6a). Moreover, the multiple comparisons test shows significant increase from control to 0.5 Gy and from 0.5 Gy to 1 Gy ($p<0.01$; Fig. 6a). Pro-inflammatory microglial marker tumor necrosis factor α (TNF-α) appears to undergo a fold increase in expression ($F_{(2,23)}=11.04$, $p<0.001$; Fig. 6d). A significant increase from sham to 1 Gy ($p<.001$) and 0.5 Gy to 1 Gy ($p<0.01$) is revealed by post-hoc multiple comparisons (Fig. 6d). M2 phenotype marker Chitinase-like protein 3 (Chil3) appears to undergo a trend towards significant increase in response to radiation ($F_{(2,21)}=3.45$, $p=0.0506$; Fig. 6b). Multiple comparisons shows a significant increase from 0.5 to 1 Gy ($p<0.05$; Fig. 6b) We also observed a more marked increase in repair microglia (M2) phenotype markers arginase (Arg 1) ($F_{(2,23)}=7.02$, $p<0.01$; Fig. 6c), and macrophage mannose receptor 1 (Mrc 1) ($F_{(2,21)}=16.42$, $p<0.0001$; Fig. 6e). Multiple comparisons tests show increases in Arg1 expression from control to 0.5 Gy ($p<0.05$), and from control to 1Gy ($p<0.01$; Fig. 6c). Multiple comparisons also reveal increases in Mrc 1 expression from control to 1 Gy ($p<0.0001$) and from 0.5 Gy to 1 Gy ($p<0.001$; Fig. 6e).

4. DISCUSSION

Exposure to ^{1}H resulted in significant hippocampal alterations in irradiated animals. We observed that dendritic morphology was altered by irradiation in the DG, CA1, and CA3 in measures of length, branch point, and DCI. Furthermore, irradiation generally caused a shift in proportions of dendritic spine subtypes throughout the hippocampus. ^{1}H exposure elicited changes in NMDA/AMPA receptor subunits, synaptic markers and activated microglial markers in the hippocampus. Finally, radiation appears to have increased exploratory anxiety in treated animals.

Dendrites, the arbor-like extensions protruding from the soma, play an important role in circuit formation and processing, as they must reach appropriate input targets. Changes in

dendritic structure often result in modified connections to afferents, ultimately affecting input processing within a neuron.[36] Accordingly, dendritic dysmorphia is tightly linked to impaired CNS functionality and often manifests in diseases related to cognitive abnormalities such as Down syndrome, Rett syndrome, and Autism Spectrum Disorders.[37-40] ^{1}H irradiation elicited morphological alterations throughout the hippocampus. The granular cell layer of the DG suffered a decrease in mean dendritic length and nodes only at the lower dose of 0.5 Gy. Oddly, radiation at 1 Gy increased dendritic complexity, whereas the lower dose of 0.5 Gy resulted in a decrease in complexity. The pyramidal neurons of the CA1 followed a similar pattern, showing a decrease in nodes in the basal and apical regions only at 0.5 Gy. Radiation appears to reduce the cell area in both the CA1 and CA3 only at the higher dose of 1 Gy.

Sholl analyses revealed a more significant decrease in dendritic intersections and length at 0.5 Gy than at 1 Gy, relative to sham in the DG. Changes in the DG Sholl analyses also manifested at different distances from the soma based upon dosage, where 0.5 Gy resulted in significant decreases in both intersections and arborization from 20-140 μm and 1 Gy significantly increased these values at 130-190 μm from the soma relative to sham. Sholl analyses of the CA3 reveal similar changes, where 0.5 Gy caused decreases in arborization and intersections at distances of 30-190 μm, and 1 Gy elicited increases at 110-190 μm from the soma as compared to sham. The general trend in the hippocampus is that a dosage of 0.5 Gy resulted in decreases in arborization and intersection of dendrites at closer distances from the soma (30-180 μm), and that 1 Gy resulted in increases in the same parameters at further distances from the soma (100-180 μm). The observed morphological responses suggest that total dosages cause different overall effects on neuronal morphology. Strikingly, dendritic morphology alterations in hippocampal neurons appear to be more sensitive to the lower dosage of 0.5 Gy for unknown reasons.

The ability of dendrites to reach appropriate input targets rely not only on the spatial location of individual dendrites, but also on the structures of spines—the small protrusions that cover dendrites and serve as the receptive sites for synaptic input.[41] Synaptic strength and longevity, a process dubbed long-term potentiation (LTP), is not only crucial to memory formation, but strongly dependent upon the surface area of the bulbous heads of individual spines.[42] Although spines are structurally plastic within the hippocampus, stable spines, constituting the majority of hippocampal spines, tend to persist over long periods.[43] Spines can be classified into different categories contingent upon their neck and head size. Thin spines are considered unstable because they consist of a small head and long neck. Stubby and mushroom spines, which have large head surface areas, are associated with stability, mushroom spines being the most stable due to a well-defined neck.[44] Irradiation resulted in a decrease of the number of mushroom spines in the three hippocampal subdivisions at doses of 1 Gy. The CA1 also suffered an increase in thin spines in the apical division; and at 1 Gy, the CA3 experienced a decrease in spine density in the basal division. Interestingly, no changes in spines were observed at 0.5 Gy.

The process of LTP in the glutamatergic network of the hippocampus relies heavily upon the induction of NMDA receptors, which upon stimulation leads to localized downstream activation of synaptic proteins, which aid in synaptic strength and maintenance.[45,46] NMDA

receptors are voltage-gated and depend upon stimulation of AMPA receptors for electric activation.[47] Lack of, or hypoactivation of NMDA receptors is linked to cognitive deficits and has been implicated in schizophrenia and Alzheimer's disease.[45] We observed that the NMDA subunit NR1 underwent a decrease in mRNA expression in the hippocampus at both treatments, with 1 Gy inducing a more pronounced effect. Fold expression of the NMDA subunit NR2A increased only at 1 Gy, an unexpected outcome, we speculate this may be a compensatory response to the decrease in NR1. The mRNA expression of the AMPA subunit, GLUR1, resulted in a decrease in both treatment groups; but was more pronounced at 1 Gy, whereas subunit GLUR2 expression decreased at only 1 Gy.

The anchoring of receptors to the actin scaffolding that defines the micromorphologies of individual spines is paramount for LTP and spine stability. Post-synaptic density protein (PSD-95) and synapse-associated protein (SAP97) are responsible for binding AMPA receptors and signaling molecules to the post-synaptic density, and their presence is crucial for normal electrical activity.[48,49] ^{1}H irradiation appears to increase SAP97 mRNA expression equally at 0.5 and 1 Gy, whereas no changes were observed in PSD-95 expression. Presynaptic markers also underwent changes in mRNA expression. Synapsin-1, essential for the regulation of presynaptic vesicle formation and clustering, significantly decreased in fold expression at a dosage of 1 Gy.[50] Low-dose radiation has been shown to elicit the immune response in the hippocampus by various measures.[16,51,52] However, Raber *et al.* have previously shown the low dose of 0.1 Gy (150MeV/n) of ^{1}H did not alter the immune response of the hippocampus significantly at 1 and 3 months postexposure.[24] Yet, our finding that ^{1}H-mediated microglia activation appears to be a dose-dependent phenomenon is consistent with this observation. Furthermore, the dose-dependent response we observed in our morphological data seems consistent with our microglial activation data, suggesting the immune response may be an important mechanism in ^{1}H-induced dendritic remodeling. Additionally, fold increase in mRNA expression was highest in anti-inflammatory, M2 phenotype markers Arg1 and Mrc1.[53,54]

The tri-synaptic hippocampal circuit is essential for episodic, spatial, and cognitive tasks. Input is received by the DG, which projects information to the CA3, and ultimately to the CA1, which serves as the main output.[55] Pyramidal dendrites operate as computational units and are capable of processing in both digital and analog means.[56,57] Previous studies exploring electrophysiological responses to ^{1}H irradiation found that a dosage of 1Gy (150 MeV/n) resulted in hyperpolarization of the resting potential, an increase in persistent Na^{+} current, a decrease in input resistance, and an elevated rate of miniature excitatory postsynaptic currents in CA1 neurons of mice 3-months after irradiation.[58] A different study found that 0.5 Gy of ^{1}H (150 MeV/n) effectively increased field excitatory post-synaptic potentials and reduced spontaneous oscillation frequency in the CA1 9-months postexposure in mice.[23] Finally, approximately 2-months postexposure to 0.5 Gy (150 MeV/n), mice had increased cannabinoid type 1 receptor-expressing basket cell GABA release onto pyramidal neurons, as a result of loss of tonic inhibition of GABA release.[59]

Dendritic spine and arbor instability are thought to be critically important to many psychiatric diseases such as schizophrenia, major depressive disorder, Alzheimer's disease, autism spectrum disorders, Down syndrome, Fragile X syndrome, Rett syndrome and

resulting stroke damage.[40,60] In particular, autism spectrum disorders are associated with decreased dendritic branching in the CA1 and CA4 regions of the hippocampus, schizophrenic patients show reduced dendritic branching and reduced spine density in the CA3, Alzheimer's disease presents reduced dendritic length in the apical and basal CA1, pathologies which are generally consistent with our observations.[61-63]

The ventral hippocampus plays a key role in anxiety-related behaviors. The amygdala has been shown to modulate memory consolidation in many respects.[64] Ventral hippocampus lesion studies have revealed significant reductions to height-induced anxiety in rats.[65,66] Indeed, the ventral hippocampus is enervated to and from the amygdala via the CA1.[67,68] It's possible the dendritic modulations we observed due to irradiation may have contributed significantly to inducing exploration anxiety in mice. Furthermore, morphological alterations we observed due to irradiation may have significantly compromised hippocampal circuitry.

5. CONCLUSION

NASA's PEL does not currently allow astronauts to be exposed to the radiation levels that would be encountered on a mission to Mars. Of particular concern, is the emerging paradoxical pattern of behavioral experiments demonstrating that higher dosages of ^{1}H appear to cause no behavioral deficits, whereas lower doses show deficits by various measures in rodents. It is currently unclear whether the low dose-rate encountered in a realistic mission would attenuate or exacerbate cognitive insults, as particle accelerators currently limit the amount of exposures and dose rates any study can implement. One important commonality between ^{1}H studies is that the energies used—150 MeV/n in mice, and 250 MeV/n in rats—energies just sufficient to carry particles through animals' craniums, are not representative of the energy spectrum encountered in deep space. Still, the cognitive hazards presented by deep-space radiation are alarming. The protracted cognitive insults outlined in this study demonstrate how a low-dose exposure appears more detrimental than a high-dose exposure, as seen by the more pronounced changes in morphology we observed in the 0.5 Gy cohort. There is currently only one study analyzing the effects of high-energy ^{1}H on the CNS of female rodents.[18] Impey *et al.* recently revealed ^{1}H-induced (1 Gy, 150 MeV/n) epigenetic remodeling of hippocampal neuron pathways responsible for synapse formation, neuron projection, axonogenesis, and axon guidance in a selective fashion in mice.[69] It is thus possible that the morphological alterations observed due to irradiation are dosage-dependent epigenetic responses. Future research should address sex differences in exposures, lower dose exposures to ^{1}H, multiple low-dose exposures at different energies, devote more attention to the GABAergic, inhibitory pathways, and further epigenetic research addressing different dosages.

Acknowledgements:

We thank the editor of this manuscript, Madison Hedrick, MA, of the Science Communication Group at the University of Arkansas for Medical Sciences, for her work.

Funding: This work was supported by the National Space Biomedical Research Institute (NSBRI) Grant RE03701 through NASA cooperative agreement NCC 9-58. The funders had no role in study design, data collection and

analysis, decision to publish, or preparation of the manuscript. This work was also supported by Core Facilities of the Center for Translational Neuroscience IDeA program award P30 GM110702.

REFERENCES

1. Drake Bret G., W. KD Human Exploration of Mars Design Reference Architecture 5.0. 5.0 (2014). <https://www.nasa.gov/sites/default/files/files/NASA-SP-2009-566-ADD2.pdf>.
2. Hassler DM et al. Mars' surface radiation environment measured with the Mars Science Laboratory's Curiosity rover. Science 343, 1244797, doi:10.1126/science.1244797 (2014). [PubMed: 24324275]
3. Zeitlin C et al. Measurements of energetic particle radiation in transit to Mars on the Mars Science Laboratory. Science 340, 1080–1084, doi:10.1126/science.1235989 (2013). [PubMed: 23723233]
4. National Council on Radiation Protection and Measurements. Information needed to make radiation protection recommendations for space missions beyond low-earth orbit. (National Council on Radiation Protection and Measurements, 2006).
5. Nelson GA Space Radiation and Human Exposures, A Primer. Radiation research 185, 349–358, doi:10.1667/Rr14311.1 (2016). [PubMed: 27018778]
6. Gregory Nelson LS, Janice Huff. Evidence Report: Risk of Acute and Late Central Nervous System Effects from Radiation Exposure, <https://humanresearchroadmap.nasa.gov/Evidence/reports/CNS.pdf> (2016).
7. National Council on Radiation Protection and Measurements. Radiation protection guidance for activities in low-earth orbit : recommendations of the Nattional Council on Radiation Protection and Measurements. (National Council on Radiation Protection and Measurements, 2000).
8. Cherry JD et al. Galactic cosmic radiation leads to cognitive impairment and increased abeta plaque accumulation in a mouse model of Alzheimer's disease. PloS one 7, e53275, doi:10.1371/journal.pone.0053275 (2012). [PubMed: 23300905]
9. Cameron HA & Glover LR Adult neurogenesis: beyond learning and memory. Annual review of psychology 66, 53–81, doi:10.1146/annurev-psych-010814-015006 (2015).
10. Alp M, Parihar VK, Limoli CL & Cucinotta FA Irradiation of Neurons with High-Energy Charged Particles: An In Silico Modeling Approach. PLoS computational biology 11, e1004428, doi:10.1371/journal.pcbi.1004428 (2015). [PubMed: 26252394]
11. Belov OV, Batmunkh M, Incerti S & Lkhagva O Radiation damage to neuronal cells: Simulating the energy deposition and water radiolysis in a small neural network. Physica medica : PM : an international journal devoted to the applications of physics to medicine and biology : official journal of the Italian Association of Biomedical Physics 32, 1510–1520, doi:10.1016/j.ejmp.2016.11.004 (2016).
12. Cacao E & Cucinotta FA Modeling Heavy-Ion Impairment of Hippocampal Neurogenesis after Acute and Fractionated Irradiation. Radiation research 186, 624–637, doi:10.1667/RR14569.1 (2016). [PubMed: 27925861]
13. Parihar VK et al. Cosmic radiation exposure and persistent cognitive dysfunction. Scientific reports 6, 34774, doi:10.1038/srep34774 (2016). [PubMed: 27721383]
14. Parihar VK et al. What happens to your brain on the way to Mars. Science advances 1, doi:10.1126/sciadv.1400256 (2015).
15. Allen AR, Raber J, Chakraborti A, Sharma S & Fike JR (56)Fe Irradiation Alters Spine Density and Dendritic Complexity in the Mouse Hippocampus. Radiation research 184, 586–594, doi:10.1667/RR14103.1 (2015). [PubMed: 26579941]
16. Rola R et al. Hippocampal neurogenesis and neuroinflammation after cranial irradiation with (56)Fe particles. Radiation research 169, 626–632, doi:10.1667/RR1263.1 (2008). [PubMed: 18494546]
17. Rola R et al. High-LET radiation induces inflammation and persistent changes in markers of hippocampal neurogenesis. Radiation research 164, 556–560 (2005). [PubMed: 16187787]
18. Sweet TB et al. Central nervous system effects of whole-body proton irradiation. Radiation research 182, 18–34, doi:10.1667/RR13699.1 (2014). [PubMed: 24937778]

19. Joseph JA, Hunt WA, Rabin BM & Dalton TK Possible "accelerated striatal aging" induced by 56Fe heavy-particle irradiation: implications for manned space flights. Radiation research 130, 88–93 (1992). [PubMed: 1561322]
20. Denisova NA, Shukitt-Hale B, Rabin BM & Joseph JA Brain signaling and behavioral responses induced by exposure to (56)Fe-particle radiation. Radiation research 158, 725–734 (2002). [PubMed: 12452775]
21. Michael Pecaut PH, Cara Zuccarelli, Anna Smith, Eric Zendejas, Gregory Nelson. Behavioral consequences of radiation exposure to simulated space radiation in the C57BL/6 mouse: Open field, rotorod, and acousti startle. Cognitive, Affective, & Behavioral Neuroscience 2, 329–340 (2002).
22. Parihar VK et al. Targeted overexpression of mitochondrial catalase prevents radiation-induced cognitive dysfunction. Antioxidants & redox signaling 22, 78–91, doi:10.1089/ars.2014.5929 (2015). [PubMed: 24949841]
23. Bellone JA, Rudobeck E, Hartman RE, Szucs A & Vlkolinsky R A Single Low Dose of Proton Radiation Induces Long-Term Behavioral and Electrophysiological Changes in Mice. Radiation research 184, 193–202 (2015). [PubMed: 26207690]
24. Raber J et al. Effects of Proton and Combined Proton and (56)Fe Radiation on the Hippocampus. Radiation research 185, 20–30, doi:10.1667/RR14222.1 (2016). [PubMed: 26720797]
25. Shukitt-Hale B, Szprengiel A, Pluhar J, Rabin BM & Joseph JA The effects of proton exposure on neurochemistry and behavior. Advances in space research : the official journal of the Committee on Space Research 33, 1334–1339 (2004).
26. Dulcich MS & Hartman RE Pomegranate supplementation improves affective and motor behavior in mice after radiation exposure. Evidence-based complementary and alternative medicine : eCAM 2013, 940830, doi:10.1155/2013/940830 (2013). [PubMed: 23662154]
27. Rabin BM, Buhler LL, Joseph JA, Shukitt-Hale B & Jenkins DG Effects of exposure to 56Fe particles or protons on fixed-ratio operant responding in rats. Journal of radiation research 43 Suppl, S225–228 (2002). [PubMed: 12793763]
28. Mikolaenko I, Rao LM, Roberts RC, Kolb B & Jinnah HA A Golgi study of neuronal architecture in a genetic mouse model for Lesch-Nyhan disease. Neurobiology of disease 20, 479–490, doi:10.1016/j.nbd.2005.04.005 (2005). [PubMed: 15908225]
29. Ramakers GJ et al. Dysregulation of Rho GTPases in the alphaPix/Arhgef6 mouse model of X-linked intellectual disability is paralleled by impaired structural and synaptic plasticity and cognitive deficits. Human molecular genetics 21, 268–286, doi:10.1093/hmg/ddr457 (2012). [PubMed: 21989057]
30. Titus AD et al. Hypobaric hypoxia-induced dendritic atrophy of hippocampal neurons is associated with cognitive impairment in adult rats. Neuroscience 145, 265–278, doi:10.1016/j.neuroscience.2006.11.037 (2007). [PubMed: 17222983]
31. Magarinos AM et al. Effect of brain-derived neurotrophic factor haploinsufficiency on stress-induced remodeling of hippocampal neurons. Hippocampus 21, 253–264, doi:10.1002/hipo.20744 (2011). [PubMed: 20095008]
32. Sholl DA Dendritic organization in the neurons of the visual and motor cortices of the cat. J Anat 87, 387–406 (1953). [PubMed: 13117757]
33. Morley BJ & Mervis RF Dendritic spine alterations in the hippocampus and parietal cortex of alpha7 nicotinic acetylcholine receptor knockout mice. Neuroscience 233, 54–63, doi:10.1016/j.neuroscience.2012.12.025 (2013). [PubMed: 23270857]
34. Seibenhener ML & Wooten MC Use of the Open Field Maze to measure locomotor and anxiety-like behavior in mice. Journal of visualized experiments : JoVE, e52434, doi:10.3791/52434 (2015). [PubMed: 25742564]
35. Simon P, Dupuis R & Costentin J Thigmotaxis as an index of anxiety in mice. Influence of dopaminergic transmissions. Behavioural brain research 61, 59–64 (1994). [PubMed: 7913324]
36. Tavosanis G Dendritic structural plasticity. Developmental neurobiology 72, 73–86, doi:10.1002/dneu.20951 (2012). [PubMed: 21761575]
37. Kaufmann WE & Moser HW Dendritic anomalies in disorders associated with mental retardation. Cerebral cortex 10, 981–991 (2000). [PubMed: 11007549]

38. Hutsler JJ & Zhang H Increased dendritic spine densities on cortical projection neurons in autism spectrum disorders. Brain research 1309, 83–94, doi:10.1016/j.brainres.2009.09.120 (2010). [PubMed: 19896929]
39. Jentarra GM et al. Abnormalities of cell packing density and dendritic complexity in the MeCP2 A140V mouse model of Rett syndrome/X-linked mental retardation. BMC neuroscience 11, 19, doi:10.1186/1471-2202-11-19 (2010). [PubMed: 20163734]
40. Kulkarni VA & Firestein BL The dendritic tree and brain disorders. Molecular and cellular neurosciences 50, 10–20, doi:10.1016/j.mcn.2012.03.005 (2012). [PubMed: 22465229]
41. von Bohlen Und Halbach O Structure and function of dendritic spines within the hippocampus. Annals of anatomy = Anatomischer Anzeiger : official organ of the Anatomische Gesellschaft 191, 518–531, doi:10.1016/j.aanat.2009.08.006 (2009). [PubMed: 19783417]
42. Malenka RC & Bear MF LTP and LTD: an embarrassment of riches. Neuron 44, 5–21, doi:10.1016/j.neuron.2004.09.012 (2004). [PubMed: 15450156]
43. Gu L et al. Long-term in vivo imaging of dendritic spines in the hippocampus reveals structural plasticity. The Journal of neuroscience : the official journal of the Society for Neuroscience 34, 13948–13953, doi:10.1523/JNEUROSCI.1464-14.2014 (2014). [PubMed: 25319691]
44. Bellot A et al. The structure and function of actin cytoskeleton in mature glutamatergic dendritic spines. Brain research 1573, 1–16, doi:10.1016/j.brainres.2014.05.024 (2014). [PubMed: 24854120]
45. Gonda X Basic pharmacology of NMDA receptors. Current pharmaceutical design 18, 1558–1567 (2012). [PubMed: 22280436]
46. Prybylowski K & Wenthold RJ N-Methyl-D-aspartate receptors: subunit assembly and trafficking to the synapse. The Journal of biological chemistry 279, 9673–9676, doi:10.1074/jbc.R300029200 (2004). [PubMed: 14742424]
47. Fachim HA, Pereira AC, Iyomasa-Pilon MM & Rosa ML Differential Expression of AMPA Subunits Induced by NMDA Intrahippocampal Injection in Rats. Frontiers in neuroscience 10, 32, doi:10.3389/fnins.2016.00032 (2016). [PubMed: 26912994]
48. Yudowski GA, Olsen O, Adesnik H, Marek KW & Bredt DS Acute inactivation of PSD-95 destabilizes AMPA receptors at hippocampal synapses. PloS one 8, e53965, doi:10.1371/journal.pone.0053965 (2013). [PubMed: 23342049]
49. Schluter OM, Xu W & Malenka RC Alternative N-terminal domains of PSD-95 and SAP97 govern activity-dependent regulation of synaptic AMPA receptor function. Neuron 51, 99–111, doi:10.1016/j.neuron.2006.05.016 (2006). [PubMed: 16815335]
50. Bykhovskaia M Synapsin regulation of vesicle organization and functional pools. Seminars in cell & developmental biology 22, 387–392, doi:10.1016/j.semcdb.2011.07.003 (2011). [PubMed: 21827866]
51. Poulose SM, Bielinski DF, Carrihill-Knoll K, Rabin BM & Shukitt-Hale B Exposure to 16O-particle radiation causes aging-like decrements in rats through increased oxidative stress, inflammation and loss of autophagy. Radiation research 176, 761–769 (2011). [PubMed: 21962006]
52. McBride WH, Pajonk F, Chiang CS & Sun JR NF-kappa B, cytokines, proteasomes, and low-dose radiation exposure. Military medicine 167, 66–67 (2002). [PubMed: 11873521]
53. Briken V & Mosser DM Editorial: switching on arginase in M2 macrophages. Journal of leukocyte biology 90, 839–841, doi:10.1189/jlb.0411203 (2011). [PubMed: 22045920]
54. Jablonski KA et al. Novel Markers to Delineate Murine M1 and M2 Macrophages. PloS one 10, e0145342, doi:10.1371/journal.pone.0145342 (2015). [PubMed: 26699615]
55. Wojtowicz JM Adult neurogenesis. From circuits to models. Behavioural brain research 227, 490–496, doi:10.1016/j.bbr.2011.08.013 (2012). [PubMed: 21893104]
56. Hulse BK, Moreaux LC, Lubenov EV & Siapas AG Membrane Potential Dynamics of CA1 Pyramidal Neurons during Hippocampal Ripples in Awake Mice. Neuron 89, 800–813, doi:10.1016/j.neuron.2016.01.014 (2016). [PubMed: 26889811]
57. London M, Schreibman A, Hausser M, Larkum ME & Segev I The information efficacy of a synapse. Nature neuroscience 5, 332–340, doi:10.1038/nn826 (2002). [PubMed: 11896396]

58. Sokolova IV et al. Proton radiation alters intrinsic and synaptic properties of CA1 pyramidal neurons of the mouse hippocampus. Radiation research 183, 208–218, doi:10.1667/RR13785.1 (2015). [PubMed: 25621896]
59. Lee SH et al. Neurophysiology of space travel: energetic solar particles cause cell type-specific plasticity of neurotransmission. Brain structure & function 222, 2345–2357, doi:10.1007/s00429-016-1345-3 (2017). [PubMed: 27905022]
60. Koleske AJ Molecular mechanisms of dendrite stability. Nature reviews. Neuroscience 14, 536–550, doi:10.1038/nrn3486 (2013). [PubMed: 23839597]
61. Raymond GV, Bauman ML & Kemper TL Hippocampus in autism: a Golgi analysis. Acta neuropathologica 91, 117–119 (1996). [PubMed: 8773156]
62. Kolomeets NS, Orlovskaya DD, Rachmanova VI & Uranova NA Ultrastructural alterations in hippocampal mossy fiber synapses in schizophrenia: a postmortem morphometric study. Synapse 57, 47–55, doi:10.1002/syn.20153 (2005). [PubMed: 15858835]
63. Hanks SD & Flood DG Region-specific stability of dendritic extent in normal human aging and regression in Alzheimer's disease. I. CA1 of hippocampus. Brain research 540, 63–82 (1991). [PubMed: 2054634]
64. Roozendaal B & McGaugh JL Memory modulation. Behavioral neuroscience 125, 797–824, doi:10.1037/a0026187 (2011). [PubMed: 22122145]
65. Deacon RM, Bannerman DM & Rawlins JN Anxiolytic effects of cytotoxic hippocampal lesions in rats. Behavioral neuroscience 116, 494–497 (2002). [PubMed: 12049331]
66. Treit D & Menard J Dissociations among the anxiolytic effects of septal, hippocampal, and amygdaloid lesions. Behavioral neuroscience 111, 653–658 (1997). [PubMed: 9189280]
67. Gutierrez-Castellanos N, Pardo-Bellver C, Martinez-Garcia F & Lanuza E The vomeronasal cortex - afferent and efferent projections of the posteromedial cortical nucleus of the amygdala in mice. The European journal of neuroscience 39, 141–158, doi:10.1111/ejn.12393 (2014). [PubMed: 24188795]
68. Cenquizca LA & Swanson LW Spatial organization of direct hippocampal field CA1 axonal projections to the rest of the cerebral cortex. Brain research reviews 56, 1–26, doi:10.1016/j.brainresrev.2007.05.002 (2007). [PubMed: 17559940]
69. Impey S et al. Proton irradiation induces persistent and tissue-specific DNA methylation changes in the left ventricle and hippocampus. BMC genomics 17, 273, doi:10.1186/s12864-016-2581-x (2016). [PubMed: 27036964]

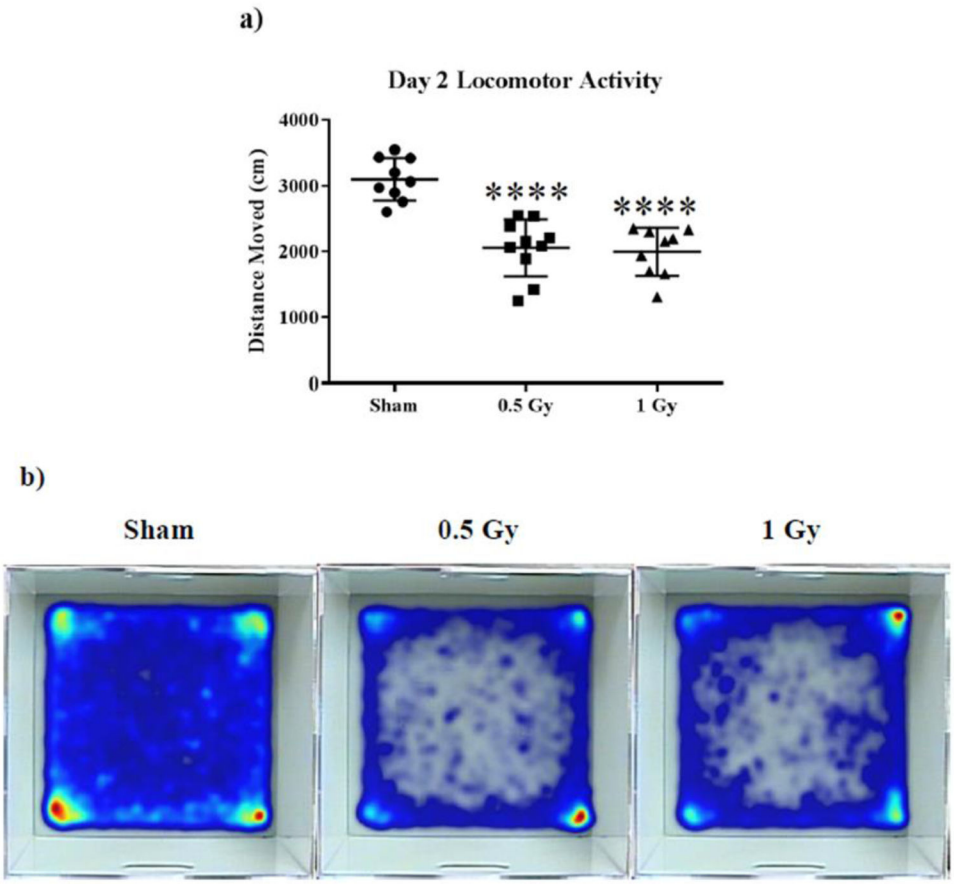

Figure 1: Open field behavior.

(A) Both irradiated groups displayed a marked reduction in total distance moved on day two. **(B)** Heat maps of average animal exploration reveal anxiety behavior in irradiated animals on open field days 1 and 2. Average ± SEM (n = 10); ****p < 0.0001.

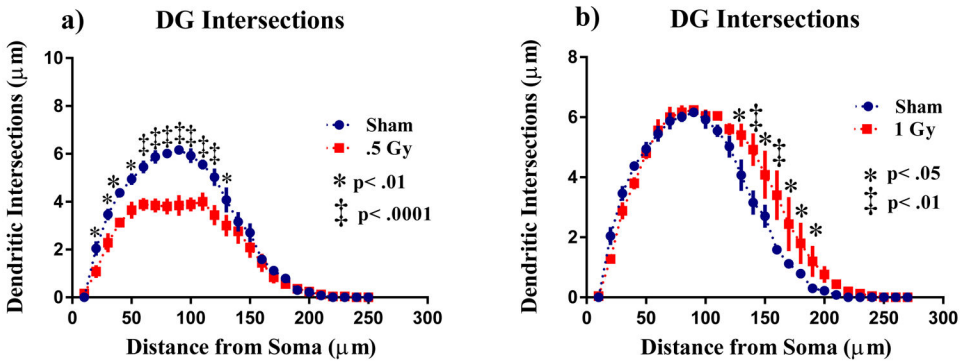

Figure 2: Sholl analyses of neurons in the dentate gyrus.

(A) Dendritic length, measured by Sholl analysis 0.5 Gy decreased arborization at 20 - 130 μm from the soma. **(B)** Surprisingly 1 Gy exposure greatly increased arborization 130 - 100 μm from the soma. Average ± SEM (n = 5); *p < 0.05.

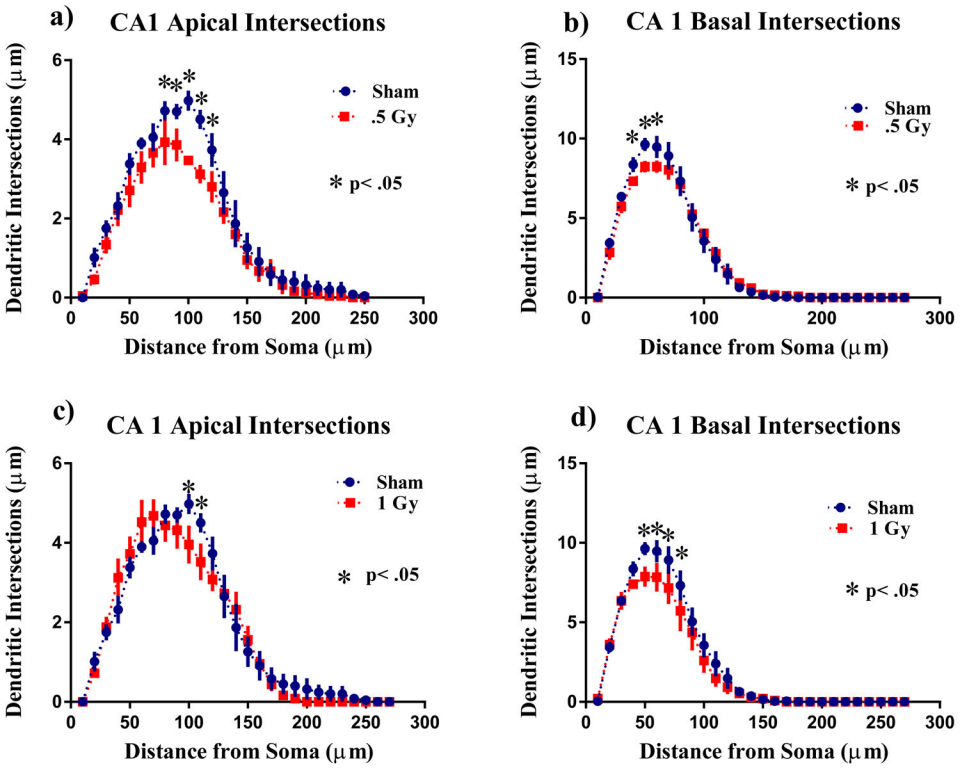

Figure 3: Sholl analyses of CA1 pyramidal neurons.

a) Sholl analysis revealed that 0.5 Gy irradiation significantly decreased intersections at 80–120 µm in CA1 apical pyramidal dendrites. b) In the basal dendrites there was a decrease in dendritic arborization 40 - 60 µm away from the soma. c) In the apical dendrites 1 Gy irradiation significantly decreased intersections 120 - 130 µm from the soma. d) In the basal dendrites 1 Gy irradiation decreased intersections 50 - 80µm from the soma Average ± SEM (n = 5); *p < 0.05

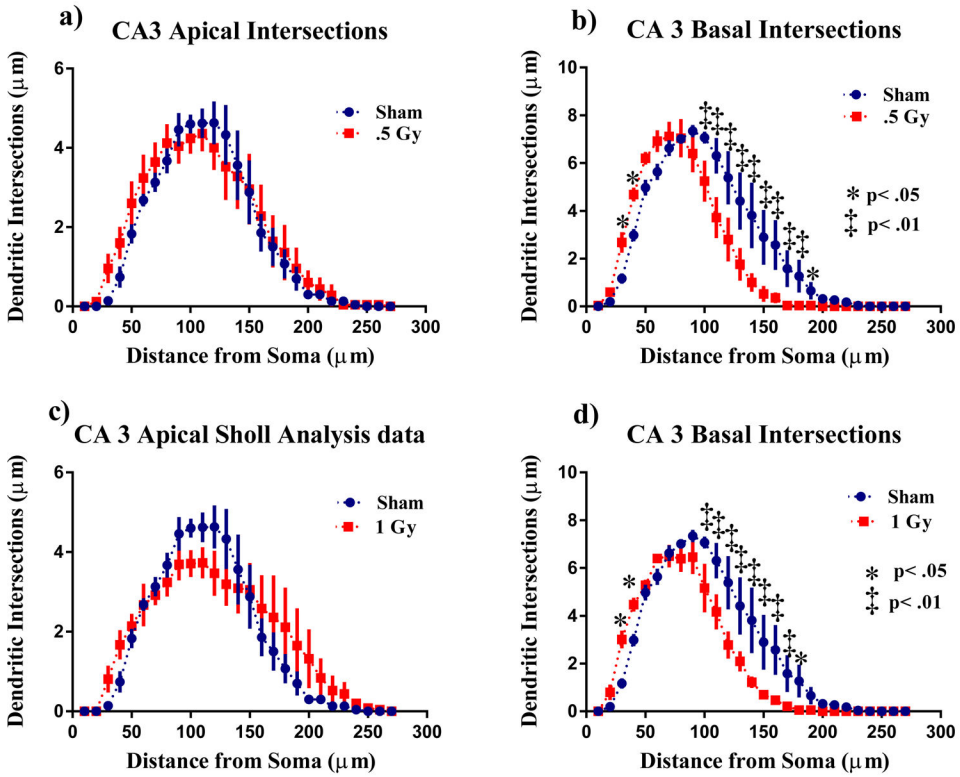

Figure 4: Sholl analyses of CA3 pyramidal neurons.

a) 0.5Gy radiation did not affect arborization in CA3 apical pyramidal dendrites. b) In the basal dendrites there was a decrease dendritic arborization 30 - 40 µm and 100 - 210 µm away from the soma. c) In the apical dendrites 1 Gy irradiation did not affect arborization. d) In the basal dendrites 1 Gy irradiation decreased intersections 30 - 40µm and 100 - 180µm from the soma Average ± SEM (n = 6); *p < 0.05

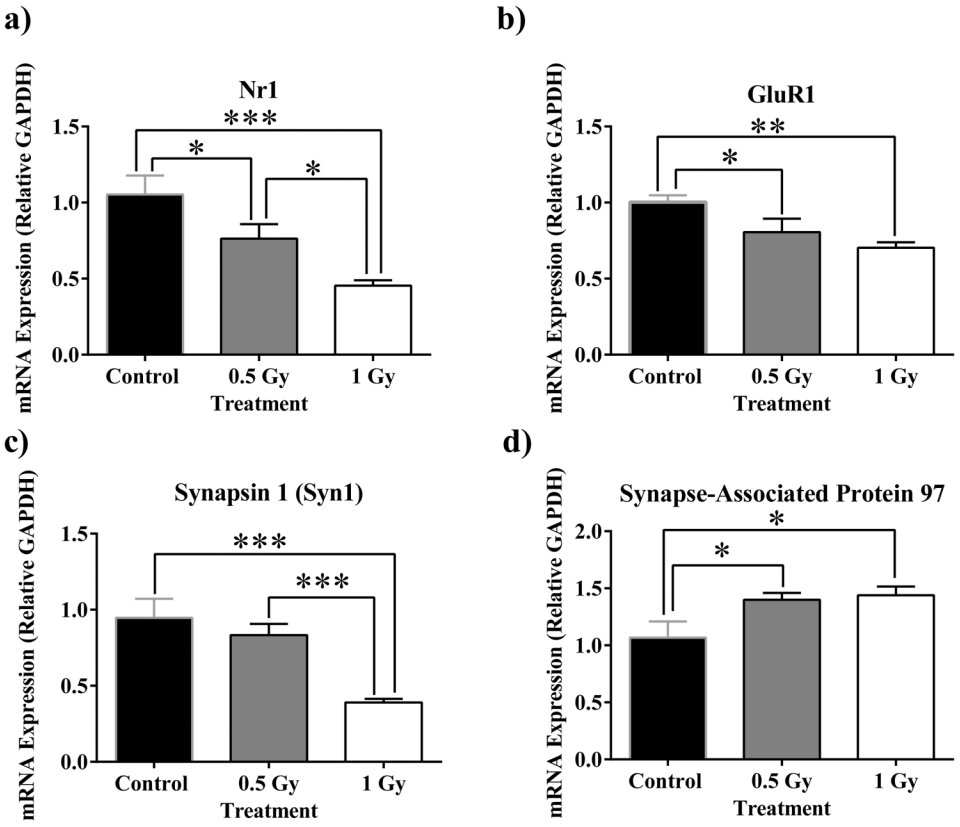

Figure 5: Alterations in NMDA/AMPA subunit (a and b), and synaptic marker (c and d) mRNA expression.

a) NMDA receptor subunit NR1 undergoes dose-dependent fold reduction. b) ^{1}H irradiation induces reduction in expression of AMPA receptor subunit GluR. c) Presynaptic vesicle trafficking marker Synapsin 1 is down-regulated at 1 Gy. d) Postsynaptic density marker SAP-97 is up-regulated at both radiation dosages. Average ± SEM (n = 9); *p < 0.05, **p<0.01, ***p<.001.

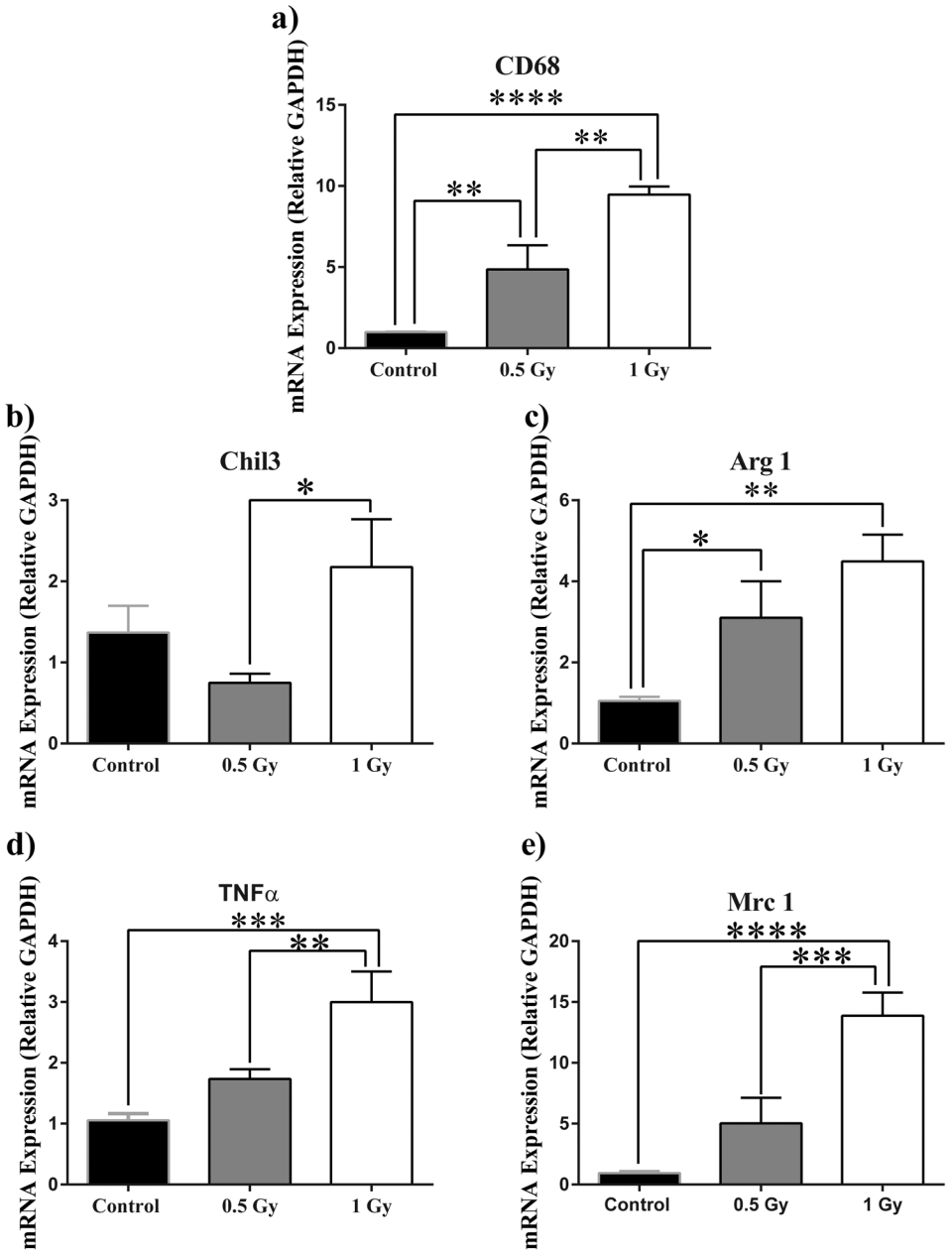

Figure 6: ^{1}H radiation up-regulates microglial mRNA markers.

a) Activated microglia increasead in a dose-dependent manner . b) M2 marker Chil3 showed a marked increase in up-regulation from 0.5 Gy to 1 Gy treatment. c) M2 phenotypic marker Arg1 expression significantly increased at 0.5 Gy and more so at 1 Gy. A dosage of 1 Gy induced significant fold increases of pro-inflammatory TNF-α (d) and M2 marker Mrc 1 (e). Average ± SEM (n = 9); *p < 0.05, **p<0.01, ***p<.001, ****p<0.0001.

Table 1:

Effects of ^{1}H on spine Morphology in the Hippocampal DG

Cell Type and Measurement	0 Gy (mean ± SEM)	.5 Gy (mean ± SEM)	1 Gy (mean ± SEM)
DG			
Thin Spines	57.99 ± 0.73	54.29 ± 1.18	56.95 ± 1.63
Stubby Spines	30.46 ± 1.50	***34.69 ± 1.01***	32.55 ± 0.97
Mushroom Spines	12.37 ± 1.03	11.02 ± 0.58	***8.12 ± 0.43***

****Bold figures represent significant values

Table 2:

Effects of ^{1}H on Spine Morphology in the Hippocampal CA 1

Cell Type and Measurement	0 Gy (mean ± SEM)	.5 Gy (mean ± SEM)	1 Gy (mean ± SEM)
CA1 Apical			
Thin Spines	52.27 ± 1.89	55.86 ± 0.83	***61.10 ± 1.87***
Stubby Spines	36.27 ± 2.37	33.70 ± 1.45	31.64 ± 1.66
Mushroom Spines	11.46 ± 1.44	10.43 ± 0.78	***7.33 ± 0.67***

Cell Type and Measurement	0 Gy (mean ± SEM)	.5 Gy (mean ± SEM)	1 Gy (mean ± SEM)
CA1 Basal			
Thin Spines	54.39 ± 0.91	52.69 ± 1.00	59.82 ± 2.72
Stubby Spines	30.13 ± 0.96	34.66 ± 1.81	31.81 ± 2.19
Mushroom Spines	12.29 ± 1.10	10.78 ± 0.17	***8.36 ± 0.74***

****Bold figures represent significant values

Table 3:

Effects of ^{1}H on Spine Morphology in the Hippocampal CA 3

Cell Type and Measurement	0 Gy (mean ± SEM)	.5 Gy (mean ± SEM)	1 Gy (mean ± SEM)
CA3 Apical			
Thin Spines	58.33 ± 0.91	54.17 ± 2.60	56.81 ± 1.32
Stubby Spines	30.80 ± 1.60	34.43 ± 2.91	35.52 ± 1.36
Mushroom Spines	12.30 ± 1.42	11.40 ± 0.70	***7.66 ± 0.28***

Cell Type and Measurement	0 Gy (mean ± SEM)	.5 Gy (mean ± SEM)	1 Gy (mean ± SEM)
CA3 Basal			
Thin Spines	57.41 ± 1.44	52.65 ± 2.74	57.19 ± 0.71
Stubby Spines	30.16 ± 2.00	34.94 ± 2.71	33.34 ± 0.76
Mushroom Spines	12.43 ± 1.64	10.06 ± 0.31	9.47 ± 0.39

****Bold figures represent significant values

Table 4:

Effects of ^{1}H on Dendrite Complexity in the Hippocampal DG

Cell Type and Measurement	0 Gy (mean ± SEM)	.5 Gy (mean ± SEM)	1 Gy (mean ± SEM)
DG			
Total Dendritic Length (μm)	871.8 ± 26.75	***626.8 ± 51.10***	1002 ± 64.72
Total # Branch Points	6.56 ± 0.20	***4.05 ± 0.05***	6.96 ± 0.37
Dendritic Complexity	18,354 ± 1,042	***8,951 ± 881***	***27,822 ± 4,334***
Cell Area	204.30 ± 17.02	231.40 ± 15.30	203.5 ± 27.16

Table 5:

Effects of ^{1}H on Dendrite Complexity in the Hippocampal CA1

Cell Type and Measurement	0 Gy (mean ± SEM)	.5 Gy (mean ± SEM)	1 Gy (mean ± SEM)
CA1 Apical			
Total Dendritic Length (μm)	671.1 ± 43.56	507.1 ± 14.44	706.8 ± 72.11
Total # Branch Points	7.34 ± 0.31	***4.71 ± 0.29***	7.79 ± 0.87
Dendritic Complexity	29,011 ± 2,477	12,207 ± 816	32,772 ± 7,732

Cell Type and Measurement	0 Gy (mean ± SEM)	.5 Gy (mean ± SEM)	1 Gy (mean ± SEM)
CA1 Basal			
Total Dendritic Length (μm)	890.6 ± 58.45	806.2 ± 46.64	758.2 ± 74.20
Total # Branch Points	9.22 ± 0.53	***6.72 ± 0.69***	6.97 ± 0.71
Dendritic Complexity	12,605 ± 1,086	10,934 ± 1,658	10,666 ± 2,462
CA1 Cell Area	279.1 ± 6.66	276.2 ± 16.25	***214.2 ± 16.92***

Table 6:

Effects of ^{1}H on Dendrite Complexity in the Hippocampal CA3

Cell Type and Measurement	0 Gy (mean ± SEM)	.5 Gy (mean ± SEM)	1 Gy (mean ± SEM)
CA3 Apical			
Total Dendritic Length (μm)	808.9 ± 24.12	663.9 ± 25.59	701.4 ± 68.76
Total # Branch Points	5.68 ± 0.17	5.40 ± 0.43	5.11 ± 0.21
Dendritic Complexity	17,130 ± 2,040	15,012 ± 3,507	14,038 ± 1,041

Cell Type and Measurement	0 Gy (mean ± SEM)	.5 Gy (mean ± SEM)	1 Gy (mean ± SEM)
CA3 Basal			
Total Dendritic Length (μm)	1029 ± 99.10	781.0 ± 50.91	781.2 ± 54.86
Total # Branch Points	7.38 ± 0.40	6.08 ± 0.42	5.85 ± 0.51
Dendritic Complexity	20,688 ± 5,411	10,708 ± 1,324	10,718 ± 2,644
Cell Area	526.3 ± 21.61	465.1 ± 24.33	***342.7 ± 9.09***

****Bold figures represent significant values